Neuron, Vol. 41, 549–561, February 19, 2004, Copyright ©2004 by Cell Press

Cell Cycle Activation Linked to Neuronal Cell Death Initiated by DNA Damage

Inna I. Kruman,[1,6,*] Robert P. Wersto,[2] Fernando Cardozo-Pelaez,[4] Lubomir Smilenov,[5] Sic L. Chan,[1] Francis J. Chrest,[2] Roland Emokpae, Jr.,[1] Myriam Gorospe,[3] and Mark P. Mattson[1,7]

[1]Laboratory of Neurosciences
[2]Research Resources Branch
[3]Laboratory of Cellular and Molecular Biology
National Institute on Aging
Intramural Research Program
5600 Nathan Shock Drive
Baltimore, Maryland 21224
[4]Department of Pharmaceutical Sciences
Center for Environmental Health Sciences
University of Montana
Missoula, Montana 59812
[5]Center of Radiology Research
Columbia University School of Medicine
630 West 168th Street
New York, New York 10032
[6]Thomas H. Christopher Center for Parkinson's Disease Research
Sun Health Research Institute
10515 West Santa Fe Drive
Sun City, Arizona 85351
[7]Department of Neuroscience
Johns Hopkins University School of Medicine
725 North Wolfe Street
Baltimore, Maryland 21205

Summary

Increasing evidence indicates that neurodegeneration involves the activation of the cell cycle machinery in postmitotic neurons. However, the purpose of these cell cycle-associated events in neuronal apoptosis remains unknown. Here we tested the hypothesis that cell cycle activation is a critical component of the DNA damage response in postmitotic neurons. Different genotoxic compounds (etoposide, methotrexate, and homocysteine) induced apoptosis accompanied by cell cycle reentry of terminally differentiated cortical neurons. In contrast, apoptosis initiated by stimuli that do not target DNA (staurosporine and colchicine) did not initiate cell cycle activation. Suppression of the function of ataxia telangiectasia mutated (ATM), a proximal component of DNA damage-induced cell cycle checkpoint pathways, attenuated both apoptosis and cell cycle reentry triggered by DNA damage but did not change the fate of neurons exposed to staurosporine and colchicine. Our data suggest that cell cycle activation is a critical element of the DNA damage response of postmitotic neurons leading to apoptosis.

*Correspondence: inna.kruman@sunhealth.org

Introduction

Recent findings suggest that neurodegeneration is associated with activation of the cell cycle machinery in postmitotic neurons (Liu and Greene, 2001; Smith et al., 2000; Copani et al., 2001). Expression of cell cycle-related proteins has been documented in neurons of patients with Alzheimer's disease (McShea et al., 1999; Nagy et al., 1998; Smith et al., 1999) and stroke (Hayashi et al., 2000) and in cultured primary neurons undergoing programmed cell death (Liu and Greene, 2001). The inhibition of cell cycle proteins such as cyclin-dependent kinases (Cdks) induces neuroprotective effects (Rideout et al., 2003). In addition, it has been shown both in vivo (Yang et al., 2001) and in vitro (Smith et al., 2000; Copani et al., 1999) that postmitotic neurons committed to cell death are able to replicate DNA. Increased mitotic indices have been associated with a variety of neurodegenerative disorders (Husseman et al., 2000). In proliferating cells, DNA damage activates the machinery responsible for DNA repair associated with cell cycle arrest, but apoptosis can result if the damage is too extensive to be repaired (Copani et al., 2001).

Recently, DNA damage has been found to activate a cell death program in terminally differentiated postmitotic neurons (Park et al., 1997). Neuroblastoma cells become extremely UV sensitive after terminal differentiation (McCombe et al., 1976). Neurons have been shown to be more vulnerable than astrocytes to DNA-damaging conditions such as ionizing radiation (Gobbel et al., 1998) and camptothecin (Morris and Geller, 1996), possibly because functionally mature neurons are generally deficient in DNA repair (Hanawalt et al., 1992). This deficiency likely contributes to a higher sensitivity of neurons to DNA damage. Thus, accumulating evidence suggests an association between DNA damage and repair, cell cycle regulation, and cell death in cycling cells (Copani et al., 2001). However, the functional role of cell cycle activation in neurons committed to cell death and the mechanisms that control the relationship between cell cycle and cell fate in terminally differentiated cells remains unclear. In the present study, we test the hypothesis that cell cycle activation in postmitotic neurons is an important component of the mechanisms involved specifically in triggering cell death initiated by DNA damage. We demonstrate that the death of cortical neurons triggered by DNA damage is associated with cell cycle reentry, in contrast to cell death initiated by nongenotoxic agents, and that blockage of the DNA damage response associated cell cycle checkpoint pathways inhibits both cell cycle activation and cell death.

Results

To study cell cycle reentry of terminally differentiated neurons, we first established cortical dissociated cultures from embryonic day 18 rats in which more than 99% of the cells express the neuron-specific microtubule-associated protein 2 (MAP-2) (Figure 1). The cul-

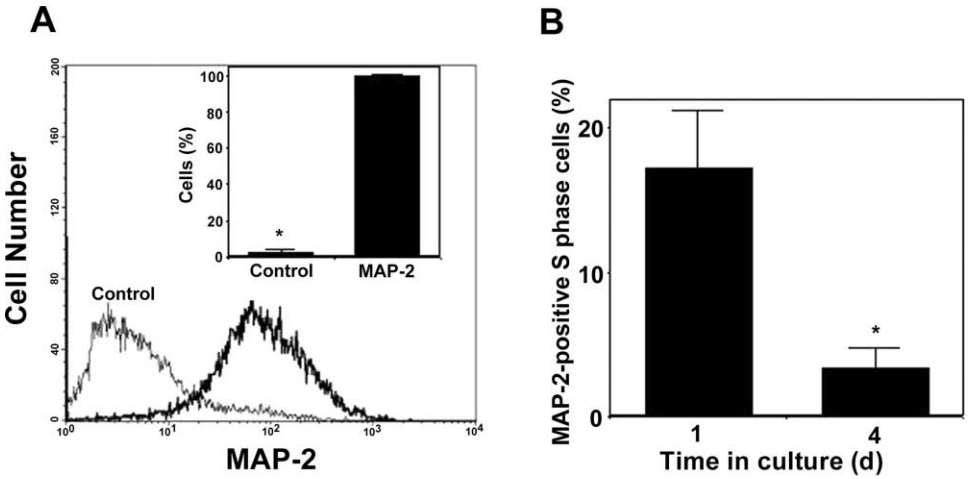

Figure 1. MAP-2 Immunostaining of Cultured Rat Cortical Neurons

(A) Immunofluorescent staining with MAP-2 antibodies quantified by flow cytometry, showing that virtually all cultured cells are MAP-2 positive. Control reflects nonspecific staining by secondary antibody alone.

(B) Cell cycle analysis of MAP-2-positive cultured cortical cells showing significant changes in their cell cycle distribution profile: the percentage of S phase cells drops from second to fourth day in culture.

tures were almost completely negative for the glial fibrillary acidic protein (GFAP) marker (data not shown). Flow cytometric analysis of cultured rat cortical neurons at increasing time points following plating showed that the percentage of MAP-2-positive S cells decreased markedly between days 1 and 4 (Figure 1B). The method of harvesting used (Copani et al., 1999) allows the high-yield isolation of viable, nondamaged cortical neurons (data not shown). We performed experiments on cells that had been in culture between 4 and 8 days, because within this time period, MAP-2-positive and GFAP-negative cultures were minimally (3%) contaminated by neuroblasts, and neurons were viable and healthy.

To test the hypothesis that cell cycle activation in postmitotic neurons is associated with DNA damage, we compared the effects of genotoxic insults that trigger apoptosis by inducing DNA damage with the effects of apoptotic insults whose actions were unrelated to genotoxicity. The genotoxic agents included the topoisomerase II inhibitor etoposide (Beck et al., 2001); homocysteine and amyloid β peptide (Aβ), both involved in pathogenesis of Alzheimer's disease (Neugroschl and Davis, 2003); and methotrexate. Methotrexate, which blocks folate metabolism and is used commonly in the treatment of cancer as a DNA-damaging agent, induces neurological abnormalities as a side effect (Ruggiero et al., 2001). Hyperhomocysteinemia and methotrexate are associated with uracil misincorporation into DNA and chromosomal breakage (Gulian et al., 1980; Blount et al., 1997), which are likely related to a chronic imbalance in DNA precursors (Van Triest et al., 2000). Homocysteine and methotrexate induce DNA damage-mediated neuronal apoptosis in vitro, as we found previously (Kruman et al., 2000, 2002). Misincorporated uracil is mainly repaired by the base excision repair (BER) system (Frosina et al., 1996). Aβ induces neuronal apoptosis in vitro (Kruman et al., 1997; Copani et al., 1999), which is likely associated with a mechanism involving oxidative DNA damage (Kruman et al., 2002). As apoptotic insults acting through mechanisms independent of genotoxicity, we employed the broad-specificity protein kinase inhibitor staurosporine and the microtubule-depolymerizing agent colchicine. Previous studies have shown that staurosporine-induced apoptosis does not involve DNA damage (Roser et al., 2001). Colchicine induces neuronal apoptosis by disrupting microtubules, which in turn triggers the release of cytochrome c from mitochondria (Uppuluri et al., 1993; Gorman et al., 1999).

DNA damage induces the production and activation of the tumor suppressor protein p53 in many cell types, including neurons (Kruman et al., 2000; Smith et al., 2003). Exposure of cultured cortical neurons to 250 μM homocysteine or 10 μM Aβ 1-42 for 14 hr resulted in an increase in the amount of p53 immunoreactivity, as assessed by confocal laser scanning microscopy (Figure 2A) and confirmed with immunoblot analyses (7 hr and 18 hr) (Figure 2B), findings that are consistent with a DNA damage response. In contrast, neurons exposed to 2 μM staurosporine displayed only a modest elevation in the intensity of p53 immunoreactive signals (Figure 2). To determine whether the cell cycle was activated in neurons exposed to DNA damaging agents, we measured levels of Cdc25A, a member of the Cdc25 gene family of dual-specificity phosphatases involved in cell cycle progression though the activation of cyclin-dependent kinases. Cdc25A is a well-established regulator of G1-to-S progression (Galaktionov et al. 1996; Donzelli et al., 2002) and marker of S phase entry. The amount of Cdc25A immunoreactivity assessed by confocal laser scanning microscopy (14 hr) and Western blotting (7 hr and 18 hr) was increased in cortical neurons exposed to homocysteine and Aβ but was unchanged in neurons exposed to staurosporine (Figure 2). Thus, expression of p53 and Cdc25A in cortical neurons following exposure to homocysteine and Aβ likely reflects the response of neurons to DNA damage and cell cycle activation, respectively.

Flow cytometry revealed a significant increase in the

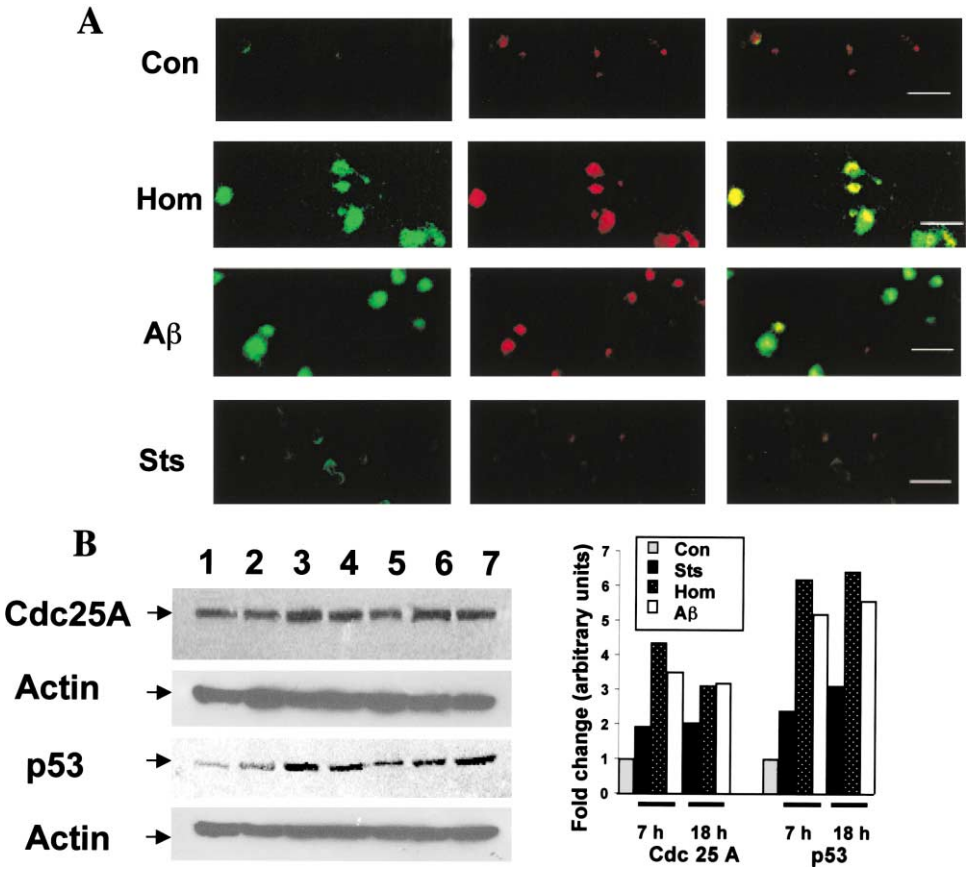

Figure 2. Homocysteine and Aβ Induce Expression of Cell Cycle- and DNA Damage-Associated Markers in Neurons

(A) Expression of p53 and Cdc25A was induced after 14 hr of continuous treatment with either 250 μM homocysteine, 10 μM Aβ, or 2 μM staurosporine. Immunoreactivity for p53 was visualized with FITC (488 nm, green), and Cdc25A was visualized with Rhodamine red (570 nm, red), with colocalization resulting in a yellow color. Strong expression of p53 and Cdc25A was seen in cortical neurons exposed to homocysteine and Aβ1-42 but not staurosporine. Scale bar, 30 μm.

(B) Immunoblots showing p53 and Cdc25 expression levels in primary cortical neurons after 7 hr (2, 3, 4) and 18 hr (5, 6, 7) of treatment with either 2 μM staurosporine (2, 5), 250 μM homocysteine (3, 6), or 10 μM Aβ (4, 7). 1, control culture. Densitometry analysis of the blots was performed using Kodak software as described in the Experimental Procedures section.

percentages of neurons in S phase in cultures exposed to different genotoxic insults, including 1 μM etoposide (20 hr), 250 μM homocysteine, 20 μM methotrexate, and 10 μM Aβ1-42 (30 hr), compared to control cultures (Figures 3A and 3B). In contrast, 2 μM staurosporine and 0.5 μM colchicine (24 hr) did not induce S phase reentry of neurons (Figures 3A and 3B). We noted a small increase in the number of neurons in G2 following staurosporine treatment, which can be explained by the fact that staurosporine induces G2/M phase arrest (Yamasaki et al., 2003). This increase (not more than 4% compared to control) can be due to the G2/M arrest in about 3% of the cycling cells present in control populations, because this increase in the percentage of G2/M cells is accompanied by a corresponding decrease in the percentage of S phase cells. In order to relate the induction of cell cycle progression to DNA damage and cell death, we quantified DNA damage (DNA strand breaks) using the comet assay (Kruman et al., 2002) and apoptosis by counting cells with apoptotic nuclei in cultures stained with Hoechst dye. As expected, each of these insults induced apoptosis (Figure 3C). However, whereas homocysteine, methotrexate, Aβ1-42, and etoposide induced DNA damage within 5 hr of treatment (long before any substantial increases in apoptotic death were seen), staurosporine and colchicine did not (Figure 3D). There was no evidence of DNA damage in neurons exposed to staurosporine or colchicine for up to 10 hr (data not shown). The time of treatment and concentration for each of the apoptotic insults shown was chosen based on preliminary kinetic studies published previously (Kruman et al., 2000, 2002) or performed in the present study. Representative kinetic curves for three of the agents used are shown in Figure 4. The data suggest a causal relationship between neuronal apoptosis and cell cycle activation in cultures of cortical neurons exposed to 2 μM staurosporine, 0.5 μM colchicine, or 1 μM etoposide for increasing periods of time. At the designated time points, apoptotic neurons were quantified by cell counts of Hoechst-stained cultures (Kruman et al., 2000), and cell cycle distribution was determined in cultures treated in parallel using flow cytometry. The percentages of apoptotic neurons and neurons in S phase in cultures exposed to etoposide

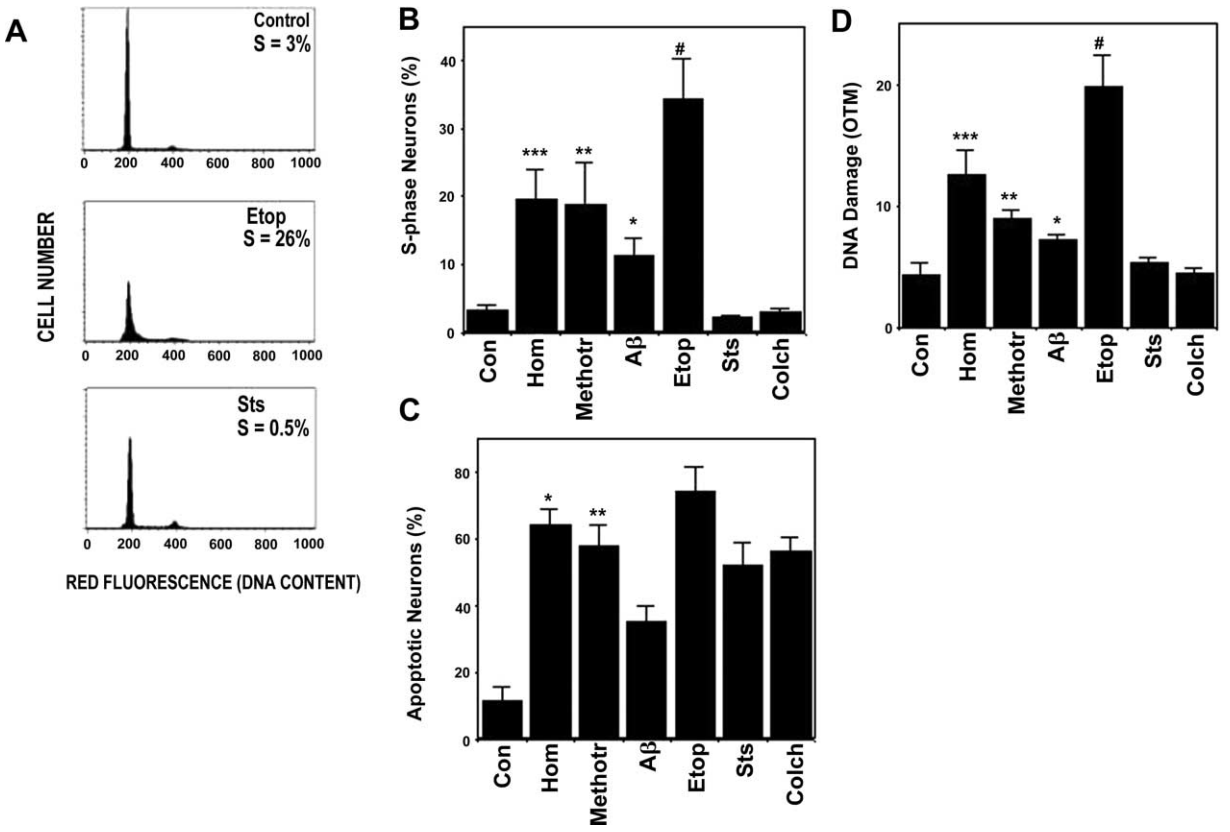

Figure 3. DNA Damage Induces DNA Replication in Postmitotic Cortical Neurons which Precedes Apoptosis

(A) Typical cell cycle distribution profiles of rat cortical neurons in control cultured cortical neurons and neurons exposed to either 1 μM etoposide or 2 μM staurosporine.

(B) Significant increase in S phase neurons following treatments with either 20 μM methotrexate, 10 μM Aβ, 250 μM homocysteine (30 hr), or 1 μM etoposide (20 hr) but not with 2 μM staurosporine or 0.5 μM colchicine (24 hr).

(C) Cultured cortical neurons were exposed for 48 hr to either 20 μM methotrexate, 10 μM Aβ, or 250 μM homocysteine, and to either 1 μM etoposide, 2 μM staurosporine, or 0.5 μM colchicine for 24 hr. All compounds induced significant apoptotic cell death.

(D) Comet assay analysis of cortical cultures treated with either 20 μM methotrexate, 250 μM homocysteine, 10 μM Aβ, or 1 μM etoposide for 5 hr reveals DNA damage in rat cortical neurons, which is expressed in OTM (Olive Tail Moment) units. Nuclei with damaged DNA have the appearance of a comet with a bright head and a tail. OTM represents the product of the amount of DNA in the tail (expressed as a percentage of the total DNA) and the distance between the centers of mass of the head and tail regions as the measure of DNA damage. Neither 2 μM staurosporine nor 0.5 μM colchicine were capable of initiating DNA damage. The values are the mean and SD ($n = 8$). *$p < 0.05$; **$p < 0.01$; ***$p < 0.001$; #$p < 0.005$ compared to control.

increased with time (Figure 4A). In contrast, staurosporine and colchicine did not initiate S phase reentry of neurons during the duration of the apoptotic process (Figure 4B).

To establish the relationship between DNA replication and apoptosis, we performed multicolor staining with apoptotic and DNA synthesis markers in the same sample preparation of cultured cortical neurons. Importantly, this analysis enables the joint assessment of G1 phase apoptotic cells as well as G2 and S phase apoptotic cells which would not be represented in the sub-G1 diploid peak (Sakakura et al., 1997). Cortical neurons were exposed to the genotoxins etoposide (1 μM; 20 hr), γ-irradiation (1 Gy; 12 hr), and Aβ (10 μM; 30 hr) or to the nongenotoxic agent staurosporine (2 μM; 24 hr), each in combination with the DNA precursor bromodeoxyuridine (10 μM; BrdU). Terminal deoxynucleotide transferase dUTP Nick End Labeling (TUNEL, which labels apoptotic nuclei) and DNA replication analysis were performed in cells counterstained with 7-aminoactinomycin D (7-AAD) to relate apoptosis to cell cycle position or DNA ploidy. This approach is based on the differential labeling of apoptosis-associated DNA strand breaks versus the photolytically generated BrdU-associated DNA strand breaks (Li et al., 1996). The results of the flow cytometric analysis revealed a significant percentage of apoptotic neurons and neurons that had incorporated BrdU due to DNA replication in cultures treated with a classical DNA damaging agent, γ-irradiation, as well as the genotoxic agents etoposide and Aβ, indicating that the neurons underwent apoptosis during or after S phase transition (Figures 5B–5D). Neuronal cultures treated with the nongenotoxic agent staurosporine contained apoptotic cells, but very few were BrdU positive, indicating lower rates of DNA synthesis in this population (Figure 5). These data show that DNA replication is linked to neuronal apoptosis initiated by DNA damage.

To better define the molecular cascade involved in the DNA damage response of postmitotic neurons that

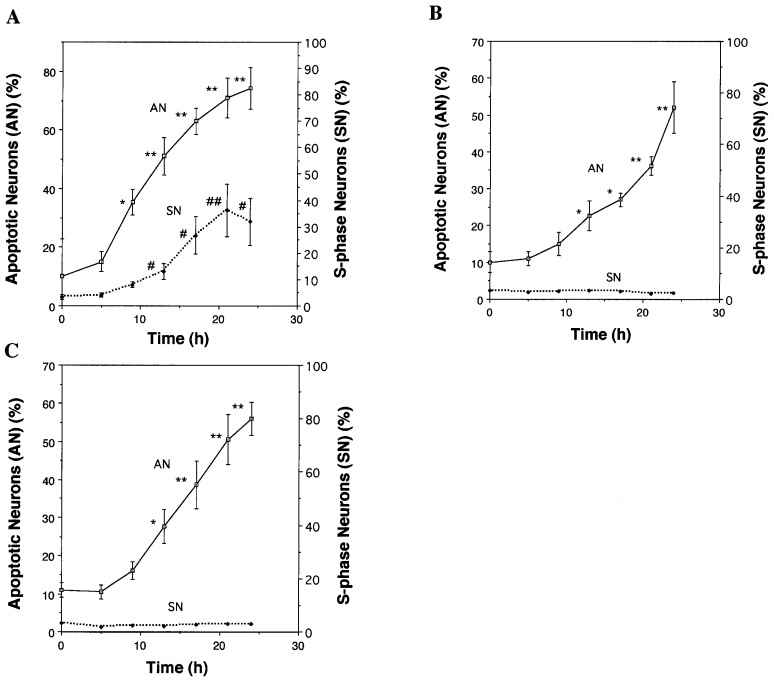

Figure 4. Apoptosis Mediated by Etoposide but Not by Staurosporine or Colchicine Is Accompanied by Cell Cycle Progression

Cultured cortical neurons were exposed to either 1 μM etoposide (A), 2 μM staurosporine (B), or 0.5 μM colchicine (C) during the indicated periods of time. The dynamics of apoptosis and percentage of S phase neurons in the cell populations exposed to 1 μM etoposide, 2 μM staurosporine, and 0.5 μM colchicine were determined. The values are the mean and SD ($n = 6$). *$p < 0.01$; **$p < 0.001$; #$p < 0.05$; ##$p < 0.002$.

results in cell cycle reentry and culminates in apoptosis, we employed strategies to inhibit the function of a pivotal mediator of genotoxic stress, the ataxia-telangiectasia mutated (ATM) protein, a proximal component of DNA damage-induced cell cycle checkpoint pathways (Rotman and Shiloh, 1998). Pretreatment with 20 mM caffeine, which directly inhibits ATM kinase activity (Savitsky et al., 1995; Sarkaria et al., 1999; Blasina et al., 1999), protected cultured cortical neurons against apoptosis induced by 1 μM etoposide (Figures 6A and 6B) and inhibited etoposide-initiated cell cycle activation (Figure 6C). Caffeine treatment did not, however, prevent apoptosis induced by either 2 μM staurosporine (Figures 6A and 6B) or 0.5 μM colchicine (data not shown), suggesting a pivotal role for ATM in controlling the DNA damage response leading to cell cycle activation and apoptosis of postmitotic neurons. Caffeine had no effect on the extent of DNA damage in neurons exposed to etoposide (Figure 6D), consistent with an action of caffeine downstream of the DNA damage. Because ATM is a member of the phosphatidylinositol 3 (PI3)-kinase family of proteins (Savitsky et al., 1995), we employed the fungal toxin wortmannin (50 μM), a specific inhibitor of the PI-3 kinase family of enzymes, to inhibit ATM activity. Wortmannin produced the same effects as caffeine, abolishing etoposide-induced cell cycle activation and apoptosis (Figures 6B and 6C). Like caffeine, wortmannin did not prevent etoposide-induced DNA damage (Figure 6D).

Following exposure to etoposide (1 μM, 24 hr), staurosporine (2 μM, 24 hr), or Aβ1-42 (10 μM, 30 hr), neuronal apoptosis was quantified in cortical neurons derived from mice with targeted deletions in the ATM gene ($ATM^{-/-}$ mice) and from wild-type ($ATM^{+/+}$) mice, as assessed by cell counts of Hoechst-stained cultures. Embryos obtained from parental $ATM^{+/-}$ mice were dissected and processed independently. From each embryo, tissue samples were used for PCR-based genotyping. Whereas etoposide- or Aβ-induced apoptosis was significantly reduced in ATM knockout cell cultures compared with wild-type cultures, the levels of staurosporine-induced apoptosis in neurons derived from the knockout and wild-type mice were not significantly different (Figure 6E), lending additional support to the notion that ATM is essential for neuronal apoptosis initiated by DNA damage.

To determine whether DNA damage in association with cell cycle reentry plays a role in neurodegenerative processes in vivo, we employed a mouse model of Alzheimer's disease. Amyloid precursor protein (APP) mutant transgenic mice overexpressing a disease-causing mutant form of human amyloid precursor protein produce increased amounts of soluble Aβ1-42 and progressively exhibit plaque-like amyloid deposits with increasing age (Borchelt et al., 1996). We measured the levels of human Aβ1-42 and Aβ1-40 in brain tissue samples from 10-month-old APP mutant transgenic mice. No Aβ1-42 or Aβ1-40 was detected in cortical tissue homogenates from control mice, whereas, in the APP mutant mice, the levels of Aβ1-40 and Aβ1-42 in brain tissue averaged 4 and 2 nmol/gm, respectively (Figure 7A). The increased amounts of Aβ were associated with increased levels of oxo8dG, one of the most abundant DNA base lesions induced by oxidative stress (Figure 7B). To determine if deficiencies in DNA repair played a role in the increased DNA damage in the cortical cells of APP mutant mice, we determined the activity of 8-oxoguanine glycosylase 1 (mOGG1), a bifunctional glycosylase/AP lyase enzyme, which is responsible for the recognition and removal of oxo8dG as a part of the base excision repair (BER) mechanism (Wallace, 1997). Oxo8dG excision capacity (mOgg1 activity) was reduced in brain tissue of APP mutant mice compared to wild-type mice (Figure 7C), further supporting an associ-

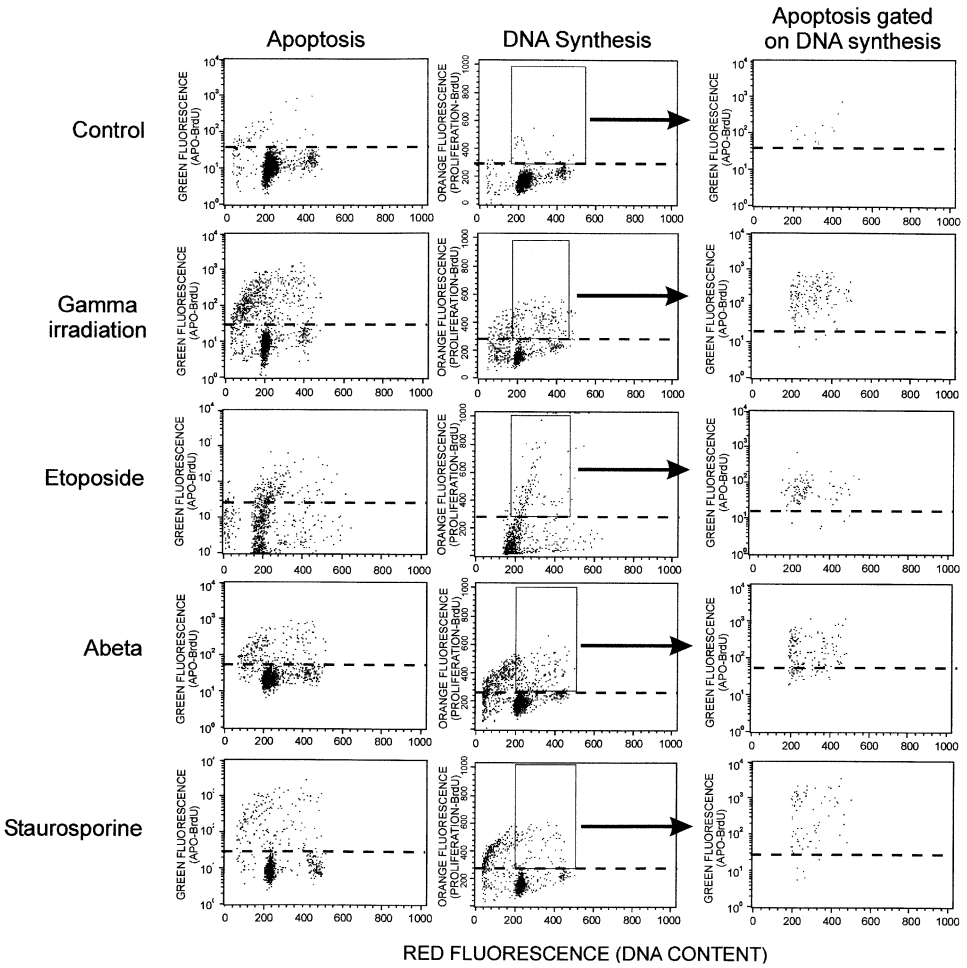

Figure 5. Simultaneous Quantification of Apoptosis and DNA Replication in Postmitotic Cortical Neurons

Cultured cortical neurons were exposed to either γ-irradiation (1 Gy, 12 hr), 1 μM etoposide (20 hr), 10 μM Aβ (30 hr), or 2 μM staurosporine (24 hr) in combination with 10 μM BrdU. DNA synthesis assay and terminal deoxynucleotide transferase dUTP Nick End Labeling (TUNEL, apoptotic assay) were performed in cells counterstained with 7-aminoactinomycin D (7-AAD) to relate apoptosis to cell cycle position or DNA ploidy. Note the significant percentage of apoptotic neurons and DNA synthesizing neurons in cultures treated with γ-irradiation, etoposide, and Aβ but not in control cultures. Staurosporine induced a significant percentage of apoptotic but not DNA synthesizing cells.

ation between increased Aβ levels and the accumulation of oxidative DNA damage in brains of APP mutant mice.

Discussion

Our findings establish a link between cell cycle activation in terminally differentiated neurons and DNA damage-induced cell death. To our knowledge, this study is the first to demonstrate that cell cycle reentry of postmitotic neurons is a critical element of the DNA damage response and that such reentry is followed by death of the neurons.

Evidence of DNA damage as a trigger of neuronal apoptosis has been documented in several neurodegenerative conditions, including ischemic and traumatic brain injuries and Alzheimer's disease (Gabbita et al., 1998; Mattson, 2000; Nagayama et al., 2000; Virag and Szabo, 2002). We found that agents that cause DNA damage by different mechanisms, including the classical DNA damage inducer γ-irradiation; the topoisomerase inhibitor etoposide; agents such as homocysteine and methotrexate, which induce genotoxic damage by causing a chronic imbalance in DNA precursors; and Aβ1-42, which causes oxidative damage of the DNA, each induced cell cycle reentry.

The transcription factor p53 has been shown to play a critical role in the DNA damage response. p53 functions include sensing damaged DNA, controlling cell cycle progression and apoptosis, and participating in DNA repair (see Almong and Rotter, 1997, for review). In the present study, we found that the levels of p53 increased in neurons exposed to homocysteine and Aβ1-42. Elevated p53 expression was previously reported in primary hippocampal neurons exposed to homocysteine (Kruman et al., 2000) and in cortical neurons exposed to Aβ (Uberti et al., 2003). Moreover, pifithrin-α, a p53 inhibitor, has been shown to protect neurons against apoptosis induced by Aβ (Culmsee et al., 2001). In our experiments, p53 overexpression in neurons exposed to homocysteine and Aβ coincided with the expression of Cdc25A,

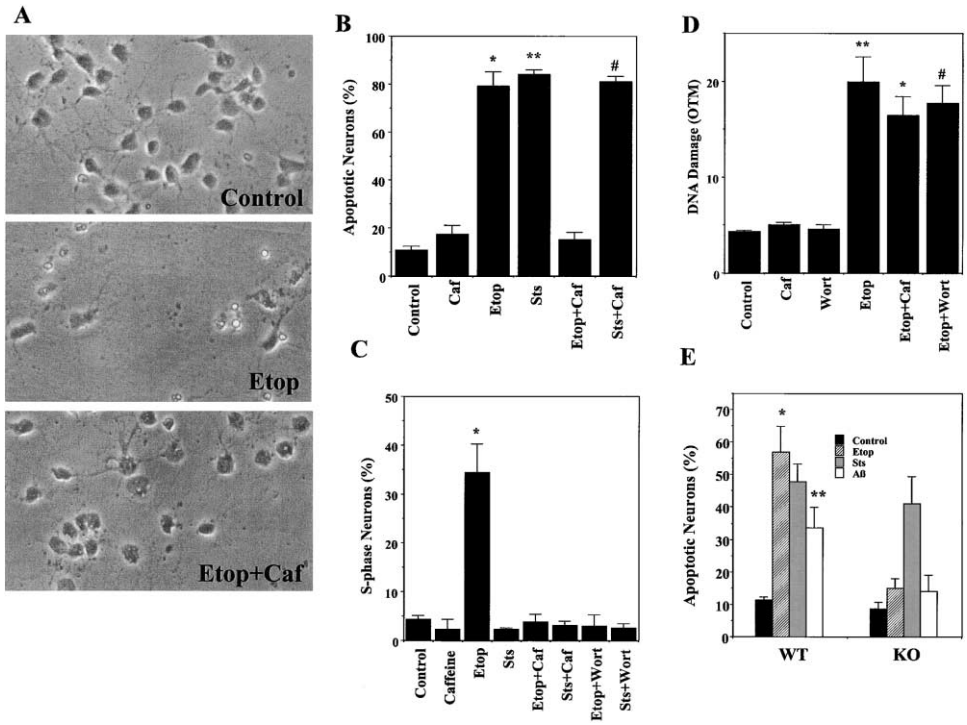

Figure 6. Suppression of ATM Function Protects Cultured Cortical Neurons Against Apoptosis and Prevents Cell Cycle Activation Induced by Etoposide

(A) Phase-contrast micrographs of cortical neurons in control culture or cultures exposed for 20 hr to either 1 μM etoposide or 1 μM etoposide + 20 mM caffeine (1 hr pretreatment).

(B) Cultured cortical neurons were exposed to 1 μM etoposide (20 hr) or 2 μM staurosporine (24 hr) alone or after 1 hr pretreatment with 20 mM caffeine or 15 min pretreatment with 50 μM wortmannin. Caffeine and wortmannin protect against neuronal apoptosis induced by etoposide but not by staurosporine.

(C) Caffeine and wortmannin prevent the cell cycle activation triggered by etoposide.

(D) Exposure of cortical neurons to 1 μM etoposide in combination with wortmannin or caffeine during 5 hr do not affect etoposide induced DNA damage.

(E) Apoptosis induced by either etoposide or Aβ but not staurosporine is reduced in neurons derived from ATM knockout ($ATM^{-/-}$) mice compared with those derived from wild-type (WT) mice. Values are the mean and SD (n = 6). *p < 0.001; **p < 0.002; #p < 0.005; ##p < 0.01.

a phosphatase that regulates entry into the S phase (Donzelli et al., 2002). In mammals, the Cdc25 family includes three homologs, Cdc25A, B, and C (Galaktionov and Beach, 1991). Cdc25A is expressed in mid-to-late G1 and induces S phase entry (Galaktionov et al., 1996). Microinjection of Cdc25A antibodies causes G1 arrest (Hoffmann et al., 1994; Cangi et al., 2000). Conversely, overexpression of Cdc25A shortens G1 phase and prematurely activates S phase (Blomberg and Hoffmann, 1999; Savitsky et al., 1999).

Cdc25A has been found to be activated in degenerating postmitotic neurons in Alzheimer's disease (Ding et al., 2000). Consistent with the expression of Cdc25A, homocysteine, and Aβ1-42, as well as other genotoxic treatments employed in the present study, including γ-irradiation, methotrexate, and etoposide, all of them induced DNA replication in postmitotic neurons. By determining the fate of BrdU-positive cells, with the BrdU having been incorporated into the DNA as the cells underwent DNA synthesis, we found that postmitotic cortical neurons exposed to different genotoxins replicate DNA (enter S phase) before undergoing cell death, suggesting that cell cycle reentry played a critical role in the death of postmitotic neurons triggered by DNA damage. In contrast, staurosporine, an agent that induced apoptosis without causing genotoxicity, did not induce cell cycle reentry and did not increase p53 or Cdc25A levels in the neurons. Likewise, the nongenotoxic colchicine did not trigger cell cycle reentry. In keeping with these findings, the suppression of cell cycle-dependent kinase (cdk) activity has been shown to produce a neuroprotective effect (Park et al., 1997, 1998; Katchanov et al., 2001; Rideout et al., 2003), possibly by perturbing the DNA damage response and associated neuronal apoptosis. Evidence in support of DNA replication events associated with S phase reentry in our experiments was obtained through the use of flow cytometry and BrdU incorporation. It is important to note that BrdU incorporation, as well as assessment of other markers like proliferating cell nuclear antigen (PCNA), may not only reveal cell cycle-associated DNA synthesis but may also serve to identify cells that have undergone DNA repair (Ninomiya et al., 1997). Obviously, complete replication of the genome during the S phase will incorporate BrdU to a much higher extent than occurs during DNA repair, and previous studies have shown that DNA repair is not a major source of BrdU labeling (Cooper-Kuhn and Kuhn, 2002). In addition, flow cytometry, a reliable method of

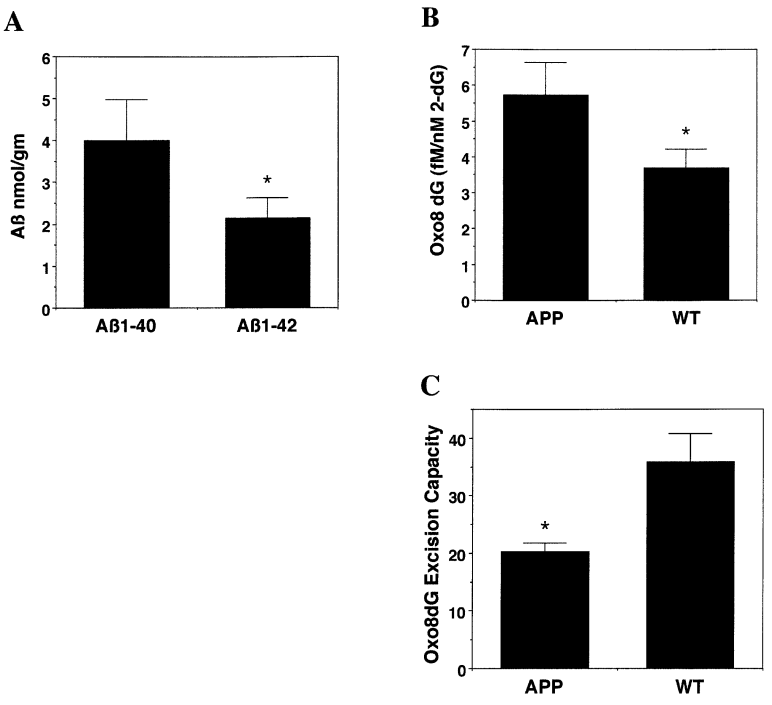

Figure 7. Transgenic Mice Bearing an APP Mutant Protein Exhibit Increased Oxidative DNA Damage

Amounts of Aβ rise markedly in 10-month-old mice. (A) Levels of Aβ1-40 and Aβ1-42 in brains of 10-month-old APP mice expressing the 695 isoform of human APP containing the double mutation Lys670->Asn, Met671->Leu were quantified by ELISA analysis. Values are the means and SE of determinations (six mice per group). (B) Levels of Oxo8dG in brains of APP and WT mice. Note the increased levels of Oxo8dG (indicative of oxidative DNA damage) in brains of APP mice. (C) Levels of Oxo8dG excision capacity (mOgg1 activity) in brains of APP and WT mice. Note the decreased levels of mOgg1 activity in brains of APP mice. Values are the mean and SD ($n = 6$). *$p < 0.01$.

cell cycle analysis that provides a quantitative assessment of DNA amount per cell, showed the G1-to-S transition in the population of cortical neurons in response to genotoxic insults in our experiments.

The involvement of the cell cycle machinery in the response of postmitotic neurons to DNA damage as a part of apoptotic mechanism was suggested by experiments in which neurons were protected against etoposide-induced toxicity when pretreated with either caffeine, an inhibitor of the DNA damage checkpoint kinase ATM (Sarkaria et al., 1999; Blasina et al., 1999), or wortmannin, an inhibitor of PI3 kinases including ATM (Savitsky et al., 1995). However, more important support for this notion comes from the discovery that primary cortical neurons derived from ATM-deficient mice were more resistant to apoptosis induced by either etoposide or Aβ than cortical neurons from the wild-type mice. In contrast, inhibition of ATM did not protect neurons against cell death induced by nongenotoxic staurosporine and colchicine. No differences in staurosporine-induced toxicity were found in our experiments with neuronal cultures derived from ATM-deficient and wild-type mice. The importance of ATM in the regulation of cell viability and genome stability is illustrated by the severe pathologies, including progressive neurodegeneration, that develop in patients with ataxia telangiectasia, a disorder caused by ATM mutation (Rotman and Shiloh, 1998). Once activated, ATM phosphorylates substrates involved in recognizing DNA damage or in signaling this damage to cell cycle checkpoints (Shiloh and Kastan, 2001). Inhibition of ATM in the present study not only protected neurons against apoptosis triggered by etoposide-induced DNA damage but also prevented S phase reentry of the cells. Blockage of ATM abrogated etoposide-induced cell cycle reentry and apoptosis but did not affect the level of DNA damage sustained, suggesting that ATM inhibition modifies the response to DNA damage. These findings reflect the intimate relationship between DNA damage-induced apoptosis and cell cycle activation in postmitotic neurons and suggests that cell cycle reentry is a requisite component of the response of postmitotic cells to DNA damage. Our results are complementary to previously published data in studies of ATM-deficient mice, which demonstrated a striking resistance of neurons to DNA damage-induced apoptosis (Herzog et al., 1998; Chong et al., 2000; Macleod et al., 2003). On the other hand, the amount of unrepaired DNA after γ-irradiation was greater in cells from ataxia-telangiectasia patients than in cells from normal individuals (Cornforth and Bedford., 1985), an observation that is consistent with our finding that ATM suppression has no effect on the amount of DNA damage caused. ATM has been shown to be necessary for neuronal apoptosis induced by γ-irradiation (Herzog et al., 1998), suggesting that ATM may function to eliminate neural cells that have incurred DNA damage.

Our results demonstrate that increased levels of soluble Aβ1-40/1-42 in brains of APP mutant transgenic mice were associated with increased levels of oxo8dG, a marker of oxidative DNA damage, and decreased activity of mOgg1, an enzyme responsible for the recognition and removal of oxo8dG (Wallace, 1997). We found that Aβ can induce DNA damage in vitro, and the damage involves oxidative DNA damage (Kruman et al., 2002), in keeping with previous reports (Culmsee et al., 2001; Uberti et al., 2003). Blockage of ATM also abrogated Aβ-induced apoptosis, further supporting the involvement of the DNA damage response in Aβ-mediated neurotoxicity. In addition, we show that Aβ treatment induces the expression of Cdc25A, a phosphatase known to be involved in regulating early cell cycle transitions and S phase progression (Galaktionov et al., 1996), and

induces the S phase reentry of cultured neurons. Similar mitotic signaling by Aβ followed by apoptosis in cultured cortical neurons has also been reported earlier (Copani et al., 1999).

Evidence of DNA damage was found in brains of Alzheimer's disease patients (Adamec et al., 1999; Lovell et al., 1999). Significantly increased levels of oxo8dG have been documented in Alzheimer's disease postmortem brain samples compared to age-matched control (Gabbita et al., 1998). On the other hand, neurons committed to cell death in the brains of Alzheimer's patients have been shown to be able to replicate DNA (Yang et al., 2001). Together with our results described here, all of these findings suggest that cell cycle activation likely represents a prerequisite step in the cascade of events triggered by the DNA damage response to Aβ in Alzheimer's disease.

In cycling cells, DNA damage results in the activation of mechanisms that arrest cell cycle progression at specific checkpoints, presumably to allow time for the damage to be repaired and thereby protecting cells from genotoxicity. However, if the damage is too extensive to be repaired, apoptosis is activated (Rhind and Russell, 2000). Alternatively, our data suggest that in postmitotic, terminally differentiated cells like neurons, DNA damage results in activation of cell cycle progression. This response may reflect the requirement of cell cycle reentry for activation of the DNA repair machinery.

Recently, physical interactions between factors involved in DNA repair and proteins known to associate with the DNA replication machinery have been described (Nagelhus et al., 1997; Otterlei et al., 1999). Various DNA repair enzymes have greater activity in proliferating than in resting cells. The expression of nuclear uracil-DNA glycosylase (UNG) has been demonstrated to be linked to cell cycle progression. UNG activity increases severalfold prior to S phase of the cell cycle (Nagelhus et al., 1997; Walsh et al., 1995). The basal activity and amount of mOgg1 protein levels were lower in differentiated compared to proliferating PC12 cells (Stedeford et al., 2001). Ku70, a subunit of the DNA-dependent protein kinase complex involved in the repair of double-stranded DNA breaks, has been observed to be expressed in extremely low levels in terminally differentiated cells (Choi et al., 2002). Global genome repair has been found to be significantly slower in differentiated neurons than in the precursor cells (Nouspikel and Hanawalt, 2000) and astrocytes. As a consequence, neurons are more vulnerable to DNA damage (Morris and Geller, 1996; Gobbel et al., 1998). However, DNA repair is critically important to the nervous system, as illustrated by the neurological abnormalities seen in patients with hereditary defects in DNA repair (Rolig and McKinnon, 2000). DNA repair pathways might be acting as a function of the cell cycle stage because DNA repair enzymes have greater activity in proliferating cells than in resting cells. The triggering of cell cycle reentry in postmitotic neurons may also contribute to apoptosis induced by DNA damage leading to the elimination of cells that have incurred DNA damage, much like in mitotic cells. Our data showing that blockage of ATM protects neurons against cell death induced by either etoposide or Aβ cell death and at the same time prevents cell cycle activation suggest that ATM and the downstream DNA repair machinery may function in conditions of an activated cell division cycle to eliminate neural cells with unrepaired DNA damage.

Experimental Procedures

Cortical Cell Cultures and Experimental Treatments

Primary cortical cell cultures were established from E18 Sprague-Dawley rats or from E16 *ATM*$^{+/-}$ (heterozygous) female mice mated with heterozygous ATM males. Mice with the ATM gene disrupted by insertion of a neo cassette (129S6/SvEvTac-*Atm*^{tm1Awb}) (Barlow et al., 1996) were maintained as a colony, and heterozygous mating pairs were used for time mating. Embryos from *ATM*$^{+/-}$ mice were dissected and processed independently. From each embryo, tissue samples were taken for PCR genotyping. The cells were plated according to procedures described earlier (Copani et al., 1999; Kruman et al., 2002). Dissociated by mild trypsination and trituration, cells were seeded onto plastic dishes or 48-well plates precoated with 0.025 mg/ml poly-L-lysine at a density of 1.3×10^3 neurons/mm^2 in Neurobasal medium containing B-27 supplement, 1 mM HEPES, 2 mM L-glutamine, and 0.001% gentamycin sulfate. Fresh medium was replaced after 30 min. All experiments were performed with 4- to 8-day-old cultures, at which time ~3% of the MAP-2-positive cells were in S phase. Aβ1-42 was purchased from Bachem (Torrance, CA) and prepared as a 1 mM solution in water 16 hr before its addition to the cell cultures at a final concentration of 10 μM. This method produces stocks that are in an early state of aggregation at the time of their addition to the cultures (Mattson et al., 1993; Fezoui et al., 2000). Homocysteine (Sigma) was prepared immediately prior to addition as a 100× stock and diluted to a final concentration of 250 μM. Methotrexate, staurosporine, colchicine, etoposide, and caffeine were purchased from Sigma. Wortmannin was purchased from Chemicon and was prepared as a concentrated stock in dimethylsulfoxide. Gamma irradiation was carried out using a Gammacell 40 Exactor research irradiator (MDS Nordion, Ontario, Canada) with a ^{137}Cs source at a specific dose rate of 1.22 Gy/min. Cells were irradiated with 1 Gy.

Assessment of Cell Survival

Apoptosis was quantified in cultures at indicated time points after exposure to experimental treatments. Cells were fixed and stained with fluorescent DNA binding dye Hoechst 33342, and the percentage of cells with apoptotic nuclei was calculated as described previously (Kruman et al., 2000).

Flow Cytometry

Flow cytometry was performed as described earlier (Copani et al., 1999; Huschtscha et al., 1994). Cultured cortical neurons were harvested following the treatments by incubation with 0.025% trypsin for 3 min. After addition of 50% fetal calf serum in HBSS salt solution, the cell suspension was centrifuged, washed with phosphate-buffered saline (PBS), and fixed in cold 70% ethanol. The harvesting of cortical cells using these conditions led to high yield of undamaged cells. For cell cycle analysis, fixed cells were washed with PBS and treated for 1 hr at 37°C with RNase (100 μg/ml) prior to propidium iodide (PI) staining (10 μg/ml in the dark for 30 min). DNA content was measured using a Becton-Dickinson FACScan flow cytometer (BD Biosciences, San Jose, CA) and cell cycle distributions analyzed using Multicycle (Phoenix Flow Systems, San Diego, CA). For immunofluorescent staining, cells were permeabilized with 0.01% (v/v) Triton X-100 and then incubated for 1 hr at 4°C with an antibody against MAP-2 (Sigma) at a dilution of 1:2000. A fluorescein (FITC)-conjugated anti-mouse IgG secondary antibody (Molecular Probes, Eugene, OR) was used to detect MAP-2 expression and was added for 30 min followed by PI for simultaneous analysis of antigen expression across the cell cycle. For the simultaneous measurement of apoptosis, DNA replication, and cellular DNA content/cell cycle by flow cytometry, the Life & Death assay (Phoenix Flow Systems, Inc.) (Li et al., 1996) was performed according to the protocol provided by the manufacturer. After treatment (1 μM etoposide, 20 hr; γ-irradiation, 1 Gy, 12 hr; 10 μM Aβ, 30 hr and 2 μM staurosporine, 24 hr) and BrdU labeling (10 μM, for the same time as the treatments), cortical cultures were harvested and fixed in

cold 70% ethanol. After washing, apoptosis-associated DNA strand breaks were end-labeled with TdT reaction buffer containing TdT enzyme and Br-dUTP for 1 hr at 37°C. Cells were washed and incubated with a fluorescein-conjugated anti-Br-dUTP antibody at room temperature for 30 min. To measure DNA replication, cells were UV-irradiated for 6 min to generate photolysis-induced DNA strand breaks associated with incorporated BrdU to make the incorporated BrdU accessible and reactive to the antibody. Cells were incubated with an anti-BrdU antibody conjugated with Phoenix Red for 30 min and counterstained with 7-aminoactinomycin D (7-AAD) for DNA content analysis. Thus, for simultaneous measurements of apoptosis and DNA replication, cells were first incubated with BrdU, which is incorporated into the DNA as the cells undergo DNA synthesis. Cells were then fixed, and apoptosis was measured using a modified TUNEL assay in which apoptotic DNA strand breaks are end-labeled with Fluorescein-conjugated BrdU using TdT. To quantify BrdU incorporated during DNA replication, DNA strand breaks were induced by photolysis only at the sites where BrdU has been incorporated during S phase. Cells were then incubated with a Phoenix Red-conjugated antibody, which then measures DNA replication. The gating was adjusted in each set of experiments using the same fluorochromes in combination or separately on the appropriate control populations (vehicle alone, mock treated, etc.).

Single-Cell Gel Electrophoresis

DNA damage was assessed using the alkaline single-cell gel electrophoresis "comet assay" method (Morris et al., 1999; Kruman et al., 2002). The comet assay has been shown to be a sensitive and reliable procedure to measure DNA strand breaks associated with incomplete excision repair sites and alkali-labile sites. Following treatment, neurons were scraped, and cell suspensions were embedded into 0.5% low melting agarose on slides (Trevigen, Gaithersburg, MD). After treatment with lysis buffer (1% Triton X-100, 10% DMSO, 2.5 M NaCl 100 mM EDTA, 10 mM Tris, pH 10), the slides were transferred to a horizontal electrophoresis unit containing the running buffer (1 mM EDTA and 0.3 M NaOH, pH 12.4), and electrophoresis was performed at 25 V and 300 mA for 30 min. The slides were then stained with ethidium bromide and analyzed using an epifluorescence microscope and the comet assay image analysis software (Komet 4.0 Kinetic Imaging LTD). Nuclei with damaged DNA have the appearance of a comet with a bright head and a tail. The tail represents the damaged DNA, which is often fragmented, and its electrophoretic mobility is consequently greater, and nuclei with undamaged DNA appear round with no tail. The Olive Tail Moment (OTM) is one of the parameters commonly used to measure comet assay data. It represents the product of the amount of DNA in the tail (expressed as a percentage of the total DNA) and the distance between the centers of mass of the head and tail regions as the measure of DNA damage.

Immunoblot Analyses

Cells were lysed in ice-cold buffer consisting of 63 mM Tris, 2 mM EDTA, 2 mM EGTA, 2% sodium dodecyl sulfate, 10% glycerol, and a protease inhibitor cocktail (Sigma, St Louis, MO), pH 6.0. Proteins (50 μg/lane) were size separated by sodium-dodecyl-sulfate-polyacrylamide gel electrophoresis (10%–15% acrylamide) and transferred to a nitrocellulose membrane. Membranes were incubated for 30 min in the presence of 5% nonfat milk and incubated overnight at 4°C with primary antibodies recognizing either phospho-p53 (S15 polyclonal antibody; 1:1000; Cell Signaling Technology, Inc., Beverly, MA), Cdc25A (Ab-3 monoclonal antibody; 1:1000; NeoMarkers, Inc., Fremont, CA), or actin. Membranes were exposed to horseradish peroxidase-conjugated secondary antibody (1:3000; Jackson Immunological Research Laboratories Inc., West Grove, PA), and immunoreactive bands were visualized using a chemiluminescence-based detection kit according to the manufacturer's protocol (ECL kit, Amersham Corp., Arlington Heights, IL). Densitometric analysis of the blots was performed using the Kodak software ID 3.5.3 USB, and intensity of the signal corrected against actin blots was expressed as a ratio of the control signals.

PCR Genotyping

DNA (10 ng) was amplified in PCR buffer II (Perkin Elmer, Boston) containing $MgCl_2$ (2.5 mM), dNTP (0.2 mM, Perkin Elmer), sucrose (8%), cresol red (0.7 mM), Taq polymerase (Perkin Elmer; 0.0167 U/μl and 0.5 μM each of 5′-CTTgggTggAgAggCTATTC-3′, 5′-AggTgAgATgACAggAgATC-3′ [neomycin cassette primers], 5′-gCTgCCATACTTgATCCATg-3′, and 5′-TCCgAA-TTTg CAggAgTTg-3′ [ATM primers flanking the neomycin cassette insertion]). After 3 min at 94°C, there were 12 cycles of 94°C (20 s), 64°C (30 s; reduced by 0.5°C every cycle), and 72°C (35 s); followed by 25 cycles of 94°C (20 s), 58°C (30 s), and 72°C (35 s); and finally by 10 min at 72°C. Products were separated by electrophoresis on 1.5% ethidium bromide-stained agarose gels and visualized under UV light. The wild-type allele produced a 147 bp product, and the disrupted allele produced a 280 bp product.

Mice and Brain Tissue Preparation

Experiments were performed in transgenic mice expressing the "Swedish" amyloid precursor protein (APP) mutation under the control of a prion promoter (Borchelt et al., 1996). The original line of mice was bred into C57BL/6 background through 19 generations. These mice develop age-dependent deposition of Aβ in their brains, which is first evident in the hippocampus and cerebral cortex beginning after 10 months of age. Ten-month-old APP mutant mice and littermate nontransgenic controls were euthanized by anesthesia overdose and decapitation. The brains were removed. One brain hemisphere was used for ELISA analysis of the levels of Aβ, and the other was used for DNA damage analysis (oxo8dG).

Quantification of 8-Oxoguanine Levels

Measurement of oxo8dG was done as described previously (Cardozo-Pelaez et al., 1998). Brain tissue and cultured cells were pulverized in liquid nitrogen using a mortar and pestle, homogenized in 10 mM of EDTA, and centrifuged. The pellet was treated with DNase-free RNase followed by digestion with proteinase K. The protein fraction was separated from DNA using three consecutive organic extractions. The first separation used phenol saturated with the extraction buffer. The second separation used phenol:chloroform:isoamyl alcohol (25:24:1), and the third separation used chloroform:isoamyl alcohol (24:1). The DNA was then precipitated out by adding two volumes of ethanol and then incubated overnight at −20°C. The purity of the DNA was determined by the absorbance of the sample at 260 nm versus 280 nm. The purified DNA was prepared for high-performance liquid chromatography analysis by resolving it into deoxynucleoside components. The amount of oxo8dG and 2-deoxyguanosine (2-dG) was calculated by comparing the peak area of oxo8dG and 2-dG obtained from the enzymatic hydrolysate of the DNA sample with a calibration curve for these compounds. The levels of oxo8dG in the samples were expressed relative to the content of 2-dG (e.g., the molar ratio of oxo8dG to 2-dG [fmol of oxo8dG/nmol of 2-dG]). Because 1 g of DNA contains 0.648 nmol of 2-dG, 1 fmol/nmol of 2-dG is equivalent to 1.54 fmol/g of DNA. The mobile phase of high-performance liquid chromatography system (HPLC) was 100 mM of sodium acetate, pH 5.2, with 5% methanol. Oxo8dG was detected by an electrochemical detector using a glassy carbon-working electrode at an applied potential of +0.4 V. 2-dG was detected in the same sample by absorbance at 260 nm. Data were recorded, stored, and analyzed with Chromatography Data System software.

Immunocytochemistry

The cultures were double immunostained with an antibody specific for p53 phosphorylated on serine 15 (S15 polyclonal antibody; 1:100; Cell Signaling Technology, Inc., Beverly, MA) and a Cdc25A antibody (Ab-3 monoclonal antibody; 1: 200 dilution; NeoMarkers, Inc., Fremont, CA), followed by an exposure to anti-rabbit IgG conjugated to FITC and anti-mouse IgG conjugated to Rhodamine (1:200 dilution; Jackson Immuno-Research, West Grove, PA). Cells were then imaged in dual-scan mode of a Zeiss CLSM 510 confocal microscope using a 40× water immersion objective.

ELISA Analysis

Solid-phase sandwich ELISAs for soluble and plaque-associated human Aβ1-42 and Aβ1-40 were performed according to a protocol provided by the manufacturer (BioSource International, Inc., Camarillo, CA). The brain tissue was homogenized in ice-cold

buffer containing 5 M guanidine HCl and 50 mM Tris-HCl, pH 8.0, and was incubated at room temperature for 3–4 hr. After dilution (1:50 v/v) with cold Dulbecco's phosphate buffered saline with 5% BSA, 0.03% Tween-20 and a cocktail of proteinase inhibitors (Calbiochem), and centrifugation, the supernatants were used for ELISA analysis.

mOgg1 Enzymatic Activity

DNA glycosylases were isolated from mouse brains as described previously (Cardozo-Pelaez et al., 2000). Briefly, tissue extracts were prepared by homogenization with buffer containing 20 mM tris, pH 8.0, 1 mM EDTA, 1 mM dithiothrietol, 0.5 mM spermine, 0.5 mM spermidine, 50% glycerol, and protease inhibitors. A volume of 2.5 M KCl (one tenth of the total homogenate volume) was added, and the samples were rocked for 30 min and centrifuged at 14,000 rpm for 30 min. The supernatant was aliquoted and stored at −70°C until time of assay. Protein levels were determined using the BCA method. Activity of mOgg1 was determined as described elsewhere (Cardozo-Pelaez et al., 2000). Briefly, a synthetic probe containing oxo8dG (Trevigen, Gaithersburg, MD) was labeled with ^{32}P at the 5′ end using polynucleotide T4 kinase (Boehringer Mannheim, Mannheim, Germany). The probe used has the following nucleotide sequence: 5′-GAACTAGTGOATCCCCCGGGCTGC-3′ (O = oxo8dG). Before the nicking reaction, this probe was annealed to its corresponding complementary oligonucleotide. The nicking reaction was carried out using 30 μg of protein extract and the double-stranded labeled probe. The reaction was carried out at 37°C for 2 hr and stopped by placing the samples in ice. These time and protein conditions were optimized to obtain values of activity that are well in the linear portion of the kinetics of the enzyme (Cardozo-Pelaez et al., 2000). Aliquots of loading buffer containing 90% formamide, 10 mM NaOH, and blue-orange dye were added to each sample. After 5 min heating at 95°C, samples were chilled and loaded into polyacrylamide gels (20%) containing 7 M urea and 1× TBE and electrophoresed at 400 mV for 2 hr. Signals were quantified using a Biorad 363 Phosphoimager system and analysis software. The capacity of the extract to remove oxo8dG was expressed as percentage of the uncleaved synthetic probe (containing oxo8dG) compared to the cleaved synthetic probe.

Statistical Analyses

Statistical analyses were performed with Microsoft Excel, and p values were obtained using ANOVA and Fisher's post hoc tests. A p value <0.05 was considered significant.

Acknowledgments

We thank Dr. A. Trzeciak, A. Lohani, and R. Baker for technical assistance; and Dr. E. Yavin for critical reading of the manuscript. This work was supported by the National Institute on Aging.

Received: May 14, 2003
Revised: September 8, 2003
Accepted: December 19, 2003
Published: February 18, 2004

References

Adamec, E., Vonsattel, J.P., and Nixon, R.A. (1999). DNA strand breaks in Alzheimer's disease. Brain Res. *849*, 67–77.

Almong, N., and Rotter, V. (1997). Involvement of p53 in cell differentiation and development. Biochim. Biophys. Acta *1333*, F1–F27.

Barlow, C., Hirotsune, S., Paylor, R., Liyanage, M., Eckhaus, M., Collins, F., Shiloh, Y., Crawley, J.N., Ried, T., Tagle, D., and Wynshaw-Boris, A. (1996). Atm-deficient mice: a paradigm of ataxia telangiectasia. Cell *86*, 159–171.

Beck, W.T., Mo, Y.Y., and Bhat, U.G. (2001). Cytotoxic signaling by inhibitors of DNA topoisomerase II. Biochem. Soc. Trans. *29*, 702–703.

Blasina, A., Price, B.D., Turenne, G.A., and McGowan, C.H. (1999). Caffeine inhibits the checkpoint kinase ATM. Curr. Biol. *9*, 1135–1138.

Blomberg, I., and Hoffmann, I. (1999). Ectopic expression of Cdc25A accelerates the G1/S transition and leads to premature activation of cyclin E- and cyclin A-dependent kinases. Mol. Cell. Biol. *19*, 6183–6194.

Blount, B.C., Mack, M.M., Wehr, C.M., MacGregor, J.T., Hiatt, R.A., Wang, G., Wickramasinghe, S.N., Everson, R.B., and Ames, B.N. (1997). Folate deficiency causes uracil misincorporation into human DNA and chromosome breakage: implication for cancer and neuronal damage. Proc. Natl. Acad. Sci. USA *94*, 3290–3295.

Borchelt, D.R., Thinakaran, G., Eckman, C.B., Lee, M.K., Davenport, F., Ratovitsky, T., Prada, C.M., Kim, G., Seekins, S., Yager, D., et al. (1996). Familial Alzheimer's disease-linked presenilin 1 variants elevate Abeta1-42/1-40 ratio in vitro and in vivo. Neuron *17*, 1005–1013.

Cangi, M.G., Cukor, B., Soung, P., Signoretti, S., Moreira, G., Jr., Ranashinge, M., Cady, B., Pagano, M., and Loda, M. (2000). Role of the Cdc25A phosphatase in human breast cancer. J. Clin. Invest. *106*, 753–761.

Cardozo-Pelaez, F., Song, S., Parthasarathy, A., Epstein, C.J., and Sanchez-Ramos, J. (1998). Attenuation of age-dependent oxidative damage to DNA and protein in brainstem of Tg Cu/Zn SOD mice. Neurobiol. Aging *19*, 311–316.

Cardozo-Pelaez, F., Brooks, P.J., Stedeford, T., Song, S., and Sanchez-Ramos, J.R. (2000). DNA damage, repair, and autooxidant systems: a correlative study. Free Radic. Biol. Med. *28*, 779–785.

Choi, E.K., Lee, Y.H., Choi, Y.S., Kwon, H.M., Choi, M.S., Ro, J.Y., Park, S.K., and Yu, E. (2002). Heterogenous expression of Ku70 in human tissues is associated with morphological and functional alterations of the nucleus. J. Pathol. *198*, 121–130.

Chong, M.J., Murray, M.R., Gosink, E.C., Russell, H.R., Srinivasan, A., Kapsetaki, M., Korsmeyer, S.J., and McKinnon, P.J. (2000). Atm and Bax cooperate in ionizing radiation-induced apoptosis in the central nervous system. Proc. Natl. Acad. Sci. USA *97*, 889–894.

Copani, A., Condorelli, F., Caruso, A., Vancheri, C., Sala, A., Giuffrida Stella, A.M., Canonico, P.L., Nicoletti, F., and Sortino, M.A. (1999). Mitotic signaling by β-amyloid causes neuronal death. FASEB J. *13*, 2225–2234.

Copani, A., Uberti, D., Sortino, M.A., Bruno, V., Nicoletti, F., and Memo, M. (2001). Activation of cell-cycle-associated proteins in neuronal death: a mandatory or dispensable path? Trends Neurosci. *24*, 25–31.

Cooper-Kuhn, C.M., and Kuhn, H.G. (2002). Is it all DNA repair? Methodological considerations for detecting neurogenesis in the adult brain. Brain Res. Dev. Brain Res. *134*, 13–21.

Cornforth, M.N., and Bedford, J.S. (1985). On the nature of a defect in cells from individuals with ataxia-telangiectasia. Science *227*, 1589–1591.

Culmsee, C., Zhu, X., Yu, Q.S., Chan, S.L., Camandola, S., Guo, Z., Greig, N.H., and Mattson, M.P. (2001). A synthetic inhibitor of p53 protects neurons against death induced by ischemic and excitotoxic insults, and amyloid beta-peptide. J. Neurochem. *77*, 220–228.

Ding, X.L., Husseman, J., Tomashevski, A., Nochlin, D., Jin, L.W., and Vincent, I. (2000). The cell cycle Cdc25A tyrosine phosphatase is activated in degenerating postmitotic neurons in Alzheimer's disease. Am. J. Pathol. *157*, 1983–1990.

Donzelli, D., Squatrito, M., Ganoth, D., Hershko, A., Pagano, M., and Draetta, F. (2002). Dual mode of degradation of Cdc25A phosphatase. EMBO J. *21*, 4875–4884.

Fezoui, Y., Hartley, D.M., Walsh, D.M., Selkoe, D.J., Osterhout, J.J., and Teplow, D.B. (2000). A *de novo* designed helix-turn-helix peptide forms nontoxic amyloid fibrils. Nat. Struct. Biol. *7*, 1095–1099.

Frosina, G., Fortini, P., Rossi, O., Carrozzino, F., Raspaglio, G., Cox, L.S., Lane, D.P., Abbondandolo, A., and Dogliotti, E. (1996). Two pathways for base excision repair in mammalian cells. J. Biol. Chem. *271*, 9573–9578.

Gabbita, S.P., Lovell, M.A., and Markesbery, W.R. (1998). Increased nuclear DNA oxidation in the brain in Alzheimer's disease. J. Neurochem. *71*, 2034–2040.

Galaktionov, K., and Beach, D. (1991). Specific activation of cdc25

tyrosine phosphatases by B-type cyclins: evidence for multiple roles of mitotic cyclins. Cell *67*, 1181–1194.

Galaktionov, K., Chen, X., and Beach, D. (1996). Cdc25 cell-cycle phosphatase as a target of c-myc. Nature *382*, 511–517.

Gobbel, G.T., Bellinzona, M., Vogt, A.R., Gupta, N., Fike, J.R., and Chan, P.H. (1998). Response of postmitotic neurons to X-irradiation: implications for the role of DNA damage in neuronal apoptosis. J. Neurosci. *18*, 147–155.

Gorman, A.M., Bonfoco, E., Zhivotovsky, B., Orrenius, S., and Ceccatelli, S. (1999). Cytochrome c release and caspase-3 activation during colchicines-induced apoptosis of cerebellar granule neurons. Eur. J. Neurosci. *11*, 1067–1072.

Gulian, M., Bleile, B., and Tseng, B.Y. (1980). Methotrexate-induced misincorporation of uracil into DNA. Proc. Natl. Acad. Sci. USA *77*, 1956–1960.

Hanawalt, P.C., Gee, P., Ho, L., Hsu, R.K., and Kane, C.J. (1992). Genomic heterogeneity of DNA repair. Role in aging? Ann. N Y Acad. Sci. *663*, 17–25.

Hayashi, T., Sakai, K., Sasaki, C., Zhang, W.R., and Abe, K. (2000). Phosphorylation of retinoblastoma protein in rat brain after transient middle cerebral artery occlusion. Neuropathol. Appl. Neurobiol. *26*, 390–397.

Herzog, K.H., Kapsetaki, M., Morgan, J.I., and McKinnon, P.J. (1998). Requirement for ATM in ionizing radiation-induced cell death in the developing central nervous system. Science *280*, 1089–1091.

Hoffmann, I., Draetta, G., and Karsenti, E. (1994). Activation of the phosphatase activity of human cdc25A by a cdk2–cyclin E dependent phosphorylation at the G1/S transition. EMBO J. *13*, 4302–4310.

Huschtscha, L.I., Jeitner, T.M., Andersson, C.E., Bartier, W.A., and Tattersall, M.H. (1994). Identification of apoptotic and necrotic human leukemic cells by flow cytometry. Exp. Cell Res. *212*, 161–165.

Husseman, J.W., Nochlin, D., and Vincent, I. (2000). Mitotic activation: A convergent mechanism for a cohort of neurodegenerative disease. Neurobiol. Aging *21*, 815–828.

Katchanov, J., Harms, C., Gertz, K., Hauck, L., Warber, C., Hirt, L., Priller, J., von Harsdorf, R., Bruck, W., Hortnagl, H., et al. (2001). Mild cerebral ischemia induces loss of cyclin-dependent kinase inhibitors and activation of cell cycle machinery before delayed neuronal cell death. J. Neurosci. *21*, 5045–5053.

Kruman, I., Bruce-Keller, A.J., Bredesen, D., Waeg, G., and Mattson, M.P. (1997). Evidence that 4-hydroxynonenal mediates oxidative stress-induced neuronal apoptosis. J. Neurosci. *17*, 5089–5100.

Kruman, I.I., Culmsee, C., Chan, S.L., Kruman, Y., Guo, Z., Penix, L., and Mattson, M.P. (2000). Homocysteine elicits a DNA damage response in neurons that promotes apoptosis and hypersensitivity to excitotoxicity. J. Neurosci. *20*, 6920–6926.

Kruman, I.I., Kumaravel, T.S., Lohani, A., Pedersen, W.A., Cutler, R.G., Kruman, Y., Haughey, N., Lee, J., Evans, M., and Mattson, M.P. (2002). Folic acid deficiency and homocysteine impair DNA repair in hippocampal neurons and sensitize them to amyloid toxicity in experimental models of Alzheimer's disease. J. Neurosci. *22*, 1752–1762.

Li, X., Melamed, M.R., and Darzynkievicz, Z. (1996). Detection of apoptosis and DNA replication by different labeling of DNA strand breaks with fluorochromes of different color. Exp. Cell Res. *222*, 28–37.

Liu, D.X., and Greene, L.A. (2001). Neuronal apoptosis at the G1/S cell cycle checkpoint. Cell Tissue Res. *305*, 217–228.

Lovell, M.A., Gabbita, S.P., and Markesbery, W.R. (1999). Increased DNA oxidation and decreased levels of repair products in Alzheimer's disease ventricular CSF. J. Neurochem. *72*, 771–776.

Macleod, M.R., Ramage, L., McGregor, A., and Seck, J.R. (2003). Reduced NMDA-induced apoptosis in neurons lacking ataxia telangiectasia mutated protein. Neuroreport *14*, 215–217.

Mattson, M.P. (2000). Apoptosis in neurodegenerative disorders. Nat. Rev. Mol. Cell Biol. *1*, 20–29.

Mattson, M.P., Tomaselli, K.J., and Rydel, R.E. (1993). Calcium-destabilizing and neurodegenerative effects of aggregated beta-amyloid peptide are attenuated by basic FGF. Brain Res. *621*, 35–49.

McCombe, P., Lavin, M., and Kidson, C. (1976). Control of DNA repair linked to neuroblastoma differentiation. Int. J. Radiat. Biol. Relat. Stud. Phys. Chem. Med. *29*, 523–531.

McShea, A., Wahl, A.F., and Smith, M.A. (1999). Re-entry into the cell cycle: a mechanism for neurodegeneration in Alzheimer disease. Med. Hypotheses *52*, 525–527.

Morris, E.J., and Geller, H.M. (1996). Induction of neuronal apoptosis by camptothecin, an inhibitor of DNA topoisomerase-I: evidence for cell cycle-independent toxicity. J. Cell Biol. *134*, 757–770.

Morris, E.J., Dreixler, J.C., Cheng, K.Y., Wilson, P.M., Gin, R.M., and Geller, H.M. (1999). Optimization of single-cell gel electrophoresis (SCGE) for quantitative analysis of neuronal DNA damage. Biotechniques *26*, 286–289.

Nagayama, T., Lan, J., Henshall, D.C., Chen, D., O'Horo, C., Simon, R.P., and Chen, J. (2000). Induction of oxidative DNA damage in the peri-infarct region after permanent focal cerebral ischemia. J. Neurochem. *75*, 1716–1728.

Nagelhus, T.A., Haug, T., Singh, K.K., Keshav, K.F., Skorpen, F., Otterlei, M., Bharati, S., Lindmo, T., Benichou, S., Benarous, R., and Krokan, H.E. (1997). A sequence in the N-terminal region of human uracil-DNA glycosylase with homology to XPA interacts with the C-terminal part of the 34-kDa subunit of replication protein A. J. Biol. Chem. *272*, 6561–6566.

Nagy, Z., Esiri, M.M., and Smith, A.D. (1998). The cell division cycle and the pathophysiology of Alzheimer's disease. Neuroscience *87*, 731–739.

Neugroschl, J., and Davis, K.L. (2003). Biological Markers in Alzheimer Disease. Am. J. Geriatr. Psychiatry *10*, 660–677.

Ninomiya, Y., Adams, R., Morris-Kay, G.M., and Eto, K. (1997). Apoptotic cell death in neuronal differentiation of P19EC cells: cell death follows reentry into S phase. J. Cell. Physiol. *172*, 25–35.

Nouspikel, T., and Hanawalt, P.C. (2000). Terminally differentiated human neurons repair transcribed genes but display attenuated global DNA repair and modulation of repair gene expression. Mol. Cell. Biol. *20*, 1562–1570.

Otterlei, M., Warbrick, E., Nagelhus, T.A., Haug, T., Slupphaug, G., Akbari, M., Aas, P.A., Steinsbekk, K., Bakke, O., and Krokan, H.E. (1999). Post-replicative base excision repair in replication foci. EMBO J. *18*, 3834–3844.

Park, D.S., Levine, B., Ferrari, G., and Greene, L. (1997). Cyclin dependent kinase inhibitors and dominant negative cyclin dependent kinase 4 and 6 promote survival of NGF-deprived sympathetic neurons. J. Neurosci. *17*, 8975–8983.

Park, D.S., Morris, E.J., Padmanabhan, J., Shelanski, M.I., Geller, H.M., and Greene, L.A. (1998). Cyclin-dependent kinases participate in death of neurons evoked by DNA-damaging agents. J. Cell Biol. *143*, 457–467.

Rhind, N., and Russell, P. (2000). Checkpoints: it takes more than time to heal some wounds. Curr. Biol. *10*, R908–R911.

Rideout, H.J., Wang, Q., Park, D.S., and Stefanis, L. (2003). Cyclin-dependent kinase activity is required for apoptotic death but not inclusion formation in cortical neurons after proteasomal inhibition. J. Neurosci. *23*, 1237–1245.

Rolig, R.L., and McKinnon, P.J. (2000). Linking DNA damage and neurodegeneration. Trends Neurosci. *23*, 417–424.

Roser, S., Pool-Zobel, B.L., and Rechkemmer, G. (2001). Contribution of apoptosis to responses in the comet assay. Mutat. Res. *497*, 169–175.

Rotman, G., and Shiloh, Y. (1998). ATM: from gene to function. Hum. Mol. Genet. *7*, 1555–1563.

Ruggiero, A., Conter, V., Milani, M., Biagi, E., Lazzareschi, I., Sparano, P., and Riccardi, R. (2001). Intrathecal chemotherapy with antineoplastic agents in children. Paediatr. Drugs *3*, 237–246.

Sakakura, C., Koide, K., Shirasu, M., Ichikawa, D., Wasaka, M., Ogaki, M., Yamazaki, J., Inazawa, J., Abe, T., Taniguchi, H., et al. (1997). Increased apoptosis rate by hyperthermochemoradiotherapy for advanced rectal cancers. Surg. Today *27*, 773–776.

Sarkaria, J.N., Busby, E.C., Tibbetts, R.S., Roos, P., Taya, Y., Karnitz,

L.M., and Abraham, R.T. (1999). Inhibition of ATM and ATR kinase by the radiosensitizing agent, caffeine. Cancer Res. *59*, 4375–4382.

Savitsky, K., Bar-Shira, A., Gilad, S., Rotman, G., Ziv, Y., Vanagaite, L., Tagle, D.A., Smith, S., Uziel, T., and Sfez, S. (1995). A single ataxia telangiectasia gene with a product similar to PI-3 kinase. Science *268*, 1749–1753.

Savitsky, K., Bar-Shira, A., Gilad, S., Rotman, G., Ziv, Y., Vanagaite, L., Tagle, D.A., Sexl, V., Diehl, J.A., Sherr, C.J., et al. (1999). A rate limiting function of cdc25A for S phase entry inversely correlates with tyrosine dephosphorylation of Cdk2. Oncogene *18*, 573–582.

Shiloh, Y., and Kastan, M.B. (2001). ATM: genome stability, neuronal development, and cancer cross paths. Adv. Cancer Res. *83*, 209–254.

Smith, M.Z., Nagy, Z., and Esiri, M.M. (1999). Cell cycle-related protein expression in vascular dementia and Alzheimer's disease. Neuroreport *271*, 45–48.

Smith, D.S., Leone, G., DeGregori, J., Ahmed, M.N., Qumsiyeh, M.B., and Nevins, J.R. (2000). Induction of DNA replication in adult rat neurons by deregulation of the retinoblastoma/E2F G1 cell cycle pathway. Cell Growth Differ. *11*, 625–633.

Smith, N.D., Rubenstein, J.N., Eggener, S.E., and Kozlowski, J.M. (2003). The p53 tumor suppressor gene and nuclear protein: basic science review and relevance in the management of bladder cancer. J. Urol. *169*, 1219–1228.

Stedeford, T., Cardozo-Pelaez, F., Nemeth, N., Song, S., Harbison, R.D., and Sanchez-Ramos, J. (2001). Comparison of base-excision repair capacity in proliferating and differentiated PC 12 cells following acute challenge with dieldrin. Free Radic. Biol. Med. *31*, 1272–1278.

Uberti, D., Ferrari Toninelli, G., and Memo, M. (2003). Involvement of DNA damage and repair systems in neurodegenerative process. Toxicol. Lett. *139*, 99–105.

Uppuluri, S., Knipling, L., Sackett, D.L., and Wolff, J. (1993). Localization of the colchicine-binding site of tubulin. Proc. Natl. Acad. Sci. USA *90*, 11598–11602.

Van Triest, B., Pinedo, H.M., Giaccone, G., and Peters, G.J. (2000). Downstream molecular determinants of response to 5-fluorouracil and antifolate thymidylate synthase inhibitors. Ann. Oncol. *11*, 385–391.

Virag, L., and Szabo, C. (2002). The therapeutic potential of poly-(ADP-ribose) polymerase inhibitors. Pharmacol. Rev. *54*, 375–429.

Wallace, S.S. (1997). Oxidative damage to DNA and its repair. In Oxidative Stress and the Molecular Biology of Antioxidant Defences, J.G. Scandalios, ed. (Cold Spring Harbor, New York: Cold Spring Harbor Laboratory), pp. 49–89.

Walsh, M.J., Shue, G., Spidoni, K., and Kapoor, A. (1995). E2F–1 and a cyclin-like DNA repair enzyme, uracil-DNA glycosylase, provide evidence for an autoregulatory mechanism for transcription. J. Biol. Chem. *270*, 5289–5298.

Yamasaki, F., Hama, S., Yoshioka, H., Kajiwara, Y., Yahara, K., Sugiyama, K., Heike, Y., Arita, K., and Kurisu, K. (2003). Staurosporine-induced apoptosis is independent of p16 and p21 and achieved via arrest at G2/M and at G1 in U251MG human glioma cell line. Cancer Chemother. Pharmacol. *51*, 271–283.

Yang, Y., Geldmacher, D.S., and Herrup, K. (2001). DNA replication precedes neuronal cell death in Alzheimer's disease. J. Neurosci. *21*, 2661–2668.